Available online at www.sciencedirect.com
ScienceDirect
International Journal of Pharmaceutics 332 (2007) 153–160
INTERNATIONAL JOURNAL OF PHARMACEUTICS
www.elsevier.com/locate/ijpharm

Pharmaceutical Nanotechnology

Evaluation of nanoparticles loaded with benzopsoralen in rat peritoneal exudate cells

A.J. Gomes [a,*], A.S. Faustino [a], C.N. Lunardi [b], L.O. Lunardi [c], A.E.H. Machado [a]

[a] *Laboratório de Fotoquímica, Instituto de Química, Universidade Federal de Uberlândia, P.O. Box 593, CEP 38400-089 Uberlândia, MG, Brazil*
[b] *Laboratório de Farmacologia, Faculdade de Ciências Farmacêuticas de Ribeirão Preto-USP, Av. Café s/n CEP 14040-903 Ribeirão Preto, SP, Brazil*
[c] *Instituto de Biociência, Universidade Estadual Júlio de Mesquita Filho, Av. 24 N1515 CEP 13506-900 Rio Claro, SP, Brazil*

Received 9 May 2005; received in revised form 28 April 2006; accepted 15 September 2006
Available online 27 September 2006

Abstract

Psoralens are widely used for the treatment of hyperproliferative skin disease. In this work, we prepared nanoparticles (NP) containing a benzopsoralen (3-ethoxy carbonyl-2*H*-benzofuro[3,2-*f*]-1-benzopiran-2-one) by the solvent evaporation technique. We evaluated important NP parameters such as particle size, drug encapsulation efficiency, effect of the encapsulation process over the drug's photochemistry, zeta potential, external morphology, and *in vitro* release behavior. We also investigated the nanoparticle as a drug delivery system (DDS), as well as its target delivery to the action site, which is a very important parameter to increase the therapeutic use of psoralens and to reduce their side effects. The uptake of benzopsoralen-loaded PLGA nanoparticles by different kinds of cells found in rat peritoneal exudates was also studied. The photodamage promoted by irradiation with UV light revealed morphological characteristics of cell damage such as cytoplasmic vesiculation, mitochondrial damage, and swelling of both the granular endoplasmatic reticulum and nuclear membrane. This encapsulation method maintained the drug's properties and improved drug delivery to the target cell.

Keywords: Benzopsoralen; Exudates peritoneal cell; Nanoparticle; PUVA

1. Introduction

The association of psoralens with ultraviolet A (UVA) irradiation (320–400 nm) is currently being employed in dermatology (orally or topically) (Makki et al., 1996; Pires et al., 2004). This combination is known as PUVA therapy (Lysenko et al., 2000; Machado et al., 2001; Canton et al., 2002; Roop et al., 2004). It has already been established that macrophages and neutrophils can be the initial target of PUVA therapy (Edelson, 1990; Okamoto et al., 1993). This treatment is effective against diseases such as vitiligo, psoriasis, mycosis fungoides, and atopic eczema, among others (Saiad et al., 1997; Tokura, 1999; Mariano et al., 2002; Tatchen et al., 2004). Unfortunately, most photosensitizing chemicals are also phototoxic to the skin, and skin contact with these molecules in the presence of UV irradiation results in sunburn, erythematic, and eventual edema (Middelkamp-Hup et al., 2004; Roop et al., 2004), thus limiting the use of PUVA therapy for the treatment of skin disorders (Lindelöf et al., 1999; Middelkamp-Hup et al., 2004). Therefore, in recent years, several highly photoreactive molecules have been synthesized aiming at developing new photochemotherapeutic drugs with fewer side effects (Machado et al., 2001; Oliveira et al., 2003; Roop et al., 2004). In this study, we evaluated the effectiveness of the compound 3-ethoxycarbonyl-2*H*-benzofuro-[3,2-*f*]-1-benzopyran-2-one (psoralen A), synthesized and kindly supplied by Oliveira-Campos (Scheme 1B) (Oliveira et al., 2003), for PUVA therapy. In this molecule, the presence of a benzene ring fused to the furan and the existence of bulky or electron-withdrawing substituents in the pyrone ring should inhibit the formation of adducts between psoralens and DNA (Machado et al., 2001; Oliveira et al., 2003). The introduction of an ester group into a benzopsoralen can furnish efficient photosensitizer derivatives, leading to high yield of singlet oxygen production (Machado et al., 2001; Llano et al., 2003). The photophysical properties of this compound have been recently investigated (Machado et al., 2001; Oliveira et al., 2003), and it has been shown that they can photochemically sensitize the generation of singlet oxygen with a quantum efficiency

* Corresponding author. Tel.: +55 34 32394143; fax: +55 34 32394208.
E-mail address: anderson@iqufu.ufu.br (A.J. Gomes).

0378-5173/$ – see front matter © 2006 Elsevier B.V. All rights reserved.
doi:10.1016/j.ijpharm.2006.09.035

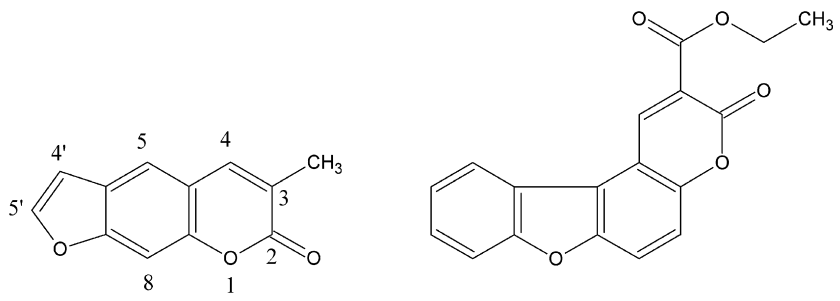

(A) (B)

Scheme 1. Representation of a typical psoralen (A) and psoralen A (3-ethoxy carbonyl-2*H*-benzofuro[3,2-*f*]-1-benzoyiran-2-one) (B).

approaching unity (Machado et al., 2001), contrary to other compounds (8-methoxypsoralen, 5-methoxypsoralen, trimethylpsoralen) (Carter et al., 1973; Cohen et al., 1981; Collins et al., 1996; Legat et al., 2001; Man et al., 2004) usually employed in PUVA therapy.

A drug delivery system (DDS) may be used to enhance the action of PUVA therapy, this is because this approach might help reduce undesirable side effects caused by psoralen, which will be directed to the target cells; *i.e.*, neutrophils and macrophages. Special interest has been focused on the use of particles prepared from polyesters like poly(DL-lactide-*co*-glycolide) (PLGA), because of their biocompatibility and biodegradability through natural pathways (Lacasse et al., 1998; Alleman et al., 1998). Recent works have described the influence of particle size and incubation time on the phagocytosis process (Panyam et al., 2003, 2004; Gomes et al., 2005), for the majority of the particles to became completely phagocyted by cells. PLGA microparticles were only phagocyted by macrophages in rat peritoneal exudate cells (Gomes et al., 2006).

In this work, we report the photophysical properties, particle size, zeta potential, and drug release profile of benzopsoralen-loaded NP. We also describe the effect of psoralen A on cells exposed to irradiation by UVA light. One of the advantages in using a DDS to carry drugs is the fact that a higher concentration of the drug can be administered. In some cases, the use of a drug in solution in the same drug concentration as used in DDS is not desirable because of this toxic effect or indiscriminate distribution through the body. The evaluation of the photobiological effects of PUVA in a DDS in the initial target cells of PUVA therapy (macrophage and neutrophyl) was carried out by employing the rat peritoneal exudate cells model. Transmission electron microscopy (TEM) helped demonstrate that the drug was entrapped in the NP and that it was able to successfully promote efficient photodamage in the target cells of PUVA therapy.

2. Materials and methods

2.1. Materials

Poly(D,L-lactic-*co*-glycolic acid) (PLGA, 50:50, Mw 17 kDa) was obtained from Sigma Chemical, Inc. (St. Louis, USA); poly(vinyl alcohol) (PVA, 13–23 kDa, 87–89% hydrolyzed) was supplied by Aldrich, (Milwaukee, USA); dichloromethane (analytical grade) was supplied by VETEC (Rio de Janeiro, Brazil). The compound 3-ethoxy carbonyl-2*H*-benzofuro[3,2-*f*]-1-benzopiran-2-one (psoralen A) was synthesized and supplied by Oliveira-Campos, from Minho University. All other chemicals were of analytical grade and used without further purification.

2.2. Methods

2.2.1. Preparation of the polymeric psoralen nanoparticle

Nanoparticles (NP) containing psoralen A were produced by the solvent evaporation technique, as described by Gomes et al. (2005). Typically, the organic phase consisted of 0.1 g of the PLGA 50:50 polymer and 10 μM psoralen A dissolved in 10 mL of CH_2Cl_2. The dispersed phase was dropped into the homogeneous aqueous phase (100 mL of an aqueous phase containing 1% (w/v) of 88% hydrolyzed PVA as dispersing agent) under ice cooling, with stirring at 15,000 rpm for 3 min, using an Ultraturrax model T25 equipped with an S25N dispersing tool (IKA Laboratory Technology, Staufen, Germany). Further solvent evaporation was carried out by gentle magnetic stirring at room temperature, for a period of 3–5 h. NP was recovered by centrifugation for 5 min, at 10,000 rpm and 4 °C. They were then washed (three times) with distilled water and lyophilized (Labconco®, USA). NP without psoralen A was prepared by the same procedure. Dried NP was stored in a sealed glass vial and placed in a desiccator kept at 4 °C.

2.2.2. Morphology of nanoparticles: SEM analysis

Surface morphology of the nanoparticles was evaluated by scanning electron microscopy (SEM). Each sample was mounted on aluminum stubs and coated with a 50 nm gold coating under argon atmosphere, because the loaded NP lacks electrical conductivity. The diameter of the NP on the SEM was then measured using a ruler, and the mean diameter was estimated using the scale on the SEM. An Electronscan ESEM 2020 (Philips Electron Optics, Eindhoven, The Netherlands) scanning electron microscope operating at 5 kV was used for these measurements.

2.2.3. Drug entrapment efficiency

The amount of psoralen A entrapped within the NP was determined spectrophotometrically (Shimadzu UV-250 1 PC) by a direct and an indirect method. The direct method involved dissolving the NP in methylene chloride and assessing drug

concentration by means of absorbance. Briefly, aliquots of the NP sample (2 mg) were dissolved in methylene chloride, and assayed in triplicate at 350 nm. The indirect method was also employed as a confirmatory assay. This was carried out by quantifying of the non-entrapped drug recovered in the external aqueous phase after NP centrifugation. Aliquots of the aqueous sample (2 mL) were evaporated to dryness by applying nitrogen purge. The solution was reconstituted by adding 2 mL of methylene chloride, and it was assayed in triplicate at 350 nm. The drug entrapment efficiency was expressed as the percentage of entrapped psoralen with respect to the total amount of drug added. The loading efficiency by direct method was calculated by means of Eq. (1):

$$\text{loading efficiency}\,(\%) = \left(\frac{L_A}{L_T}\right) \times 100 \quad (1)$$

where L_A is the amount of psoralen A in the NP and L_T is the total amount of drug added.

2.2.4. In vitro drug release

NP (10 mg) containing psoralen A was placed into falcon tubes and incubated in 10 mL release medium (Hank's buffer, pH 7.4) under magnetic stirring (150 rpm), at 37 °C. The nanosphere suspension was centrifuged every day at 10,000 rpm, for 10 min. The supernatant (10 mL) was withdrawn and replaced with 10 mL of fresh release medium. This procedure was repeated for 15 days. The amount of released psoralen was determined by measuring drug concentration in the supernatant. To determine the drug content in the supernatant, the solution was evaporated to dryness by applying nitrogen purge. The solution was reconstituted by adding 2 mL of methylene chloride to the psoralen extract, and it was assayed at 350 nm by spectrophotometry. This procedure was carried out in triplicate. The cumulative amount of psoralen release was calculated using Eq. (2):

$$\text{cumulative amount release}\,(\%) = \left(\frac{D_t}{D_\infty}\right) \times 100 \quad (2)$$

where D_t is the cumulative amount of drug (psoralen A) released at time t and D_∞ is the cumulative total amount of drug released at infinite time, which is the actual loading of the drug determined in the loading efficiency experiment.

2.2.5. Particle size and surface charge (zeta potential)

The NP surface charge and particle size were determined by photon correlation spectroscopy (PCS) using the quasi-elastic light scattering technique, on a Zetasizer 3000 equipment from Malvern Instrument (Worcstershire, UK), equipped with a 10 mW He–Ne 633-nm laser beam, at 25 °C, using a scattering angle of 90°. A dilute suspension (1.0 mg/mL) set at NP was prepared in double distilled water and sonicated in an ice bath for 30 s. The sample was subjected to particle size analysis. The NP zeta potential in 0.1 mM Hank's buffer, pH 7.4 (1.0 mg/mL), was determined using ZetaPlus™ in the zeta potential analysis mode.

2.2.6. Transmission electron microscopy (TEM) of NP in rat peritoneal exudate cell

Peritoneal exudate cells from male Wistar rats (mean weight ~150 g, $n = 6$) were used in the experiments. The rats were intraperitoneally injected with 20 mL of PBS buffer, their abdomen was massaged for 5 min to free adherent cells, and the Hank's solution was withdrawn using a syringe through a small incision made in the abdominal wall. The washing fluid was centrifuged (400 × g; 10 min), and the cell pellet was resuspensed in Hank's buffer and divided into five aliquots of 2 mL each. Time-dependent assays were carried out by incubating samples with PLGA nanospheres (100 μg/mL) for 120 min, at 37 °C. Control experiments were performed by incubating cells in the absence of NP for 120 min, at 37 °C. After incubation, the cells were washed twice with Hank's solution. For the transmission electron microscopy (TEM) studies, the samples were fixed in 2.5% glutaraldehyde in 0.1 M sodium cacodylate buffer (pH 7.4) for 2 h, at 25 °C. The fixed cells were then postfixed in 1% osmium tetroxide in the same buffer for 1 h, dehydrated in a graded acetone series, and embedded in epoxy resin. Ultrathin sections were contrasted with alcoholic 2% uranyl acetate and 5% lead citrate. Ultrastructural examination was performed with a transmission electron microscope Philips CM-100 (Philips Electron Optics, Eindhoven, The Netherlands).

2.2.7. Cell irradiation

The exudate peritoneal cells were incubated with 100 μg/mL psoralen A-loaded NP, in Hank's solution, for 120 min. The photochemical experiments were carried out using a 1-cm path-length spectrophotometric cell. A 400-W mercury arc lamp was used as the radiation source. A pass-band filter (Ocean Optics U360) filtered the radiation, ensuring irradiation of the samples with light of 360 ± 10 nm (69% of maximum transmittance). Typical irradiancies of 0.030–0.035 W/cm^2 were used to deliver a fluency of 1.0 J/cm^2. Light intensities were quantified radiometrically (Solar light model PMA 2100). After light treatment, the cells were kept in the dark for 3 h. Non-irradiated cells were kept in the dark for the same period of time. The ambient light was $<10^{-6}$ W/cm^2. Both irradiated and non-irradiated cells were processed for transmission electron microscopy.

2.2.8. Data report

Experiments were carried out in triplicate. Results are expressed as the mean with a standard deviation (S.D.), and statistical analysis was performed using a two-tailed Student's t-test.

3. Results

3.1. Preparation of PLGA nanoparticles and their morphology

Fig. 1 shows representative micrographs of psoralen A-loaded NP, magnified at 25,000×. For all preparations reported in this paper, the NP was spherical and displayed a smooth surface which was possible to observe from the external surface. No significant difference between the psoralen-containing PLGA

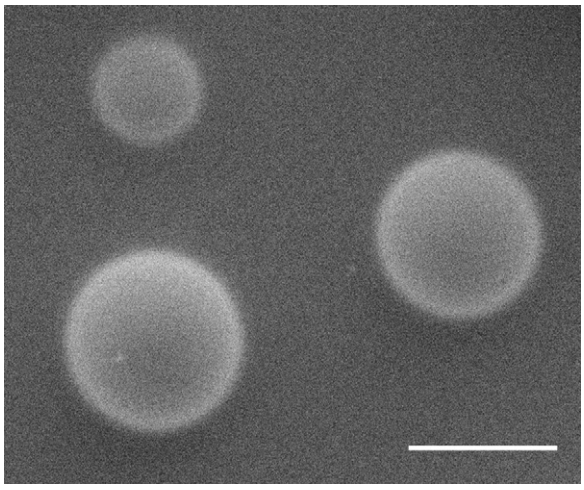

Fig. 1. Surface morphology of a psoralen A-loaded nanoparticle prepared by the solvent evaporation method. Magnification 25,000× by SEM.

nanoparticles and the empty nanoparticle used as control were found. In Fig. 1, the NPs are shown to be well-formed and they are not aggregated.

The drug entrapment efficiency parameter was calculated from the experimentally determined actual drug loading of the NP and the theoretical drug loading. The value obtained by this method was 64 (±6%) of incorporation. The values obtained by the indirect method were similar to those found via the direct method.

3.2. Particle size and surface charge (zeta potential)

The solvent evaporation method produced small particles with a mean diameter in the range of 373 nm (±62 nm), when the NP was loaded with psoralen A. When analyzed by dynamic light scattering (DLS), the NP exhibited a unimodal size distribution (Fig. 2). For all the obtained NP formulations, the polydispersity index was lower than 0.5, which was considered satisfactory. The colloidal stability was analyzed by measuring the NP zeta potential. The particles consisting of PLGA blank were negatively charged (−1.3 mV at pH 7.4), whereas the zeta potential measured for the psoralen A-loaded NP was +8.3 mV.

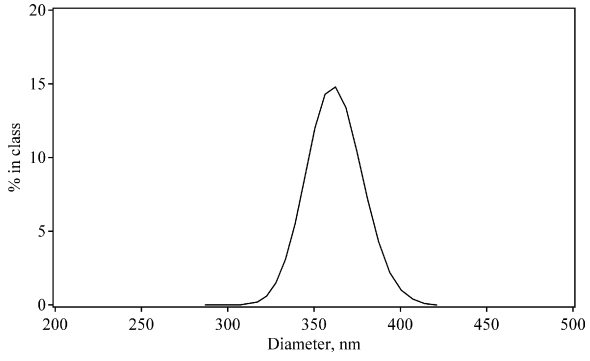

Fig. 2. Size distribution profile of nanoparticles containing psoralen A (3-ethoxy carbonyl-2*H*-benzofuro[3,2-*f*]-1-benzoyiran-2-one).

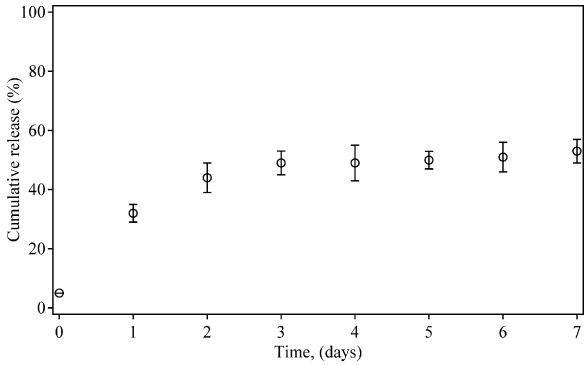

Fig. 3. Cumulative release profile of psoralen A from the PLGA nanoparticle into Hank's buffer medium (pH 7.4) after 7 days.

3.3. In vitro drug release

To optimize PUVA therapy, it is necessary to know the kinetics of drug release after application of psoralen. Therefore, we determined the day-to-day release of psoralen A into Hank's buffer in order to obtain quantitative information on the profile of psoralen A release into the disperse system, over a 15-day period. The release profile was shown for a 7-day period because the release became constant after reaching a plateau beginning on day 3 (Fig. 3).

3.4. Ultrastructure and PUVA studies

Observation of the peritoneal exudate cells in the presence of psoralen A-loaded NP by TEM showed that the NP was endocyted by the majority of the cells present in the rat cell exudate. The NP was localized near or inside the mitochondria, as observed in the macrophage cell (inset-Fig. 4A) and in the mast cell (Fig. 4C). Photodamage induced by light activation of psoralen A released from the NP was observed in all the types of cells present in the rat exudate and which phagocyted the NP. Fig. 4B and D–F shows swelling of the nuclear membrane, mitochondrial damage, and cytoplasmic vesiculation (Fig. 4D).

4. Discussion

The NP approach seems to be a promising strategy for the enhancement of therapeutic effects of drugs that are potential candidates for the treatment of several diseases (Lacasse et al., 1998; Chen and Lu, 1999; Panyam and Labhasetwar, 2003). The use of a delivery system in PUVA treatment appears to be an attractive means of protecting the drug against fast degradation. The delivery system allows sustained drug release and enables the control of some physical properties, such as drug concentration, particle size, and particle charge, thus allowing drug transport and delivery to the target cell. The morphology of the external surface of the PLGA nanoparticle obtained in this work was studied by SEM. The success of this encapsulation technique depends primarily on the retention of the hydrophobic active compound within the polymer-containing organic phase from which the matrix was formed after solvent evaporation. The entrapment values obtained with the solvent evaporation method

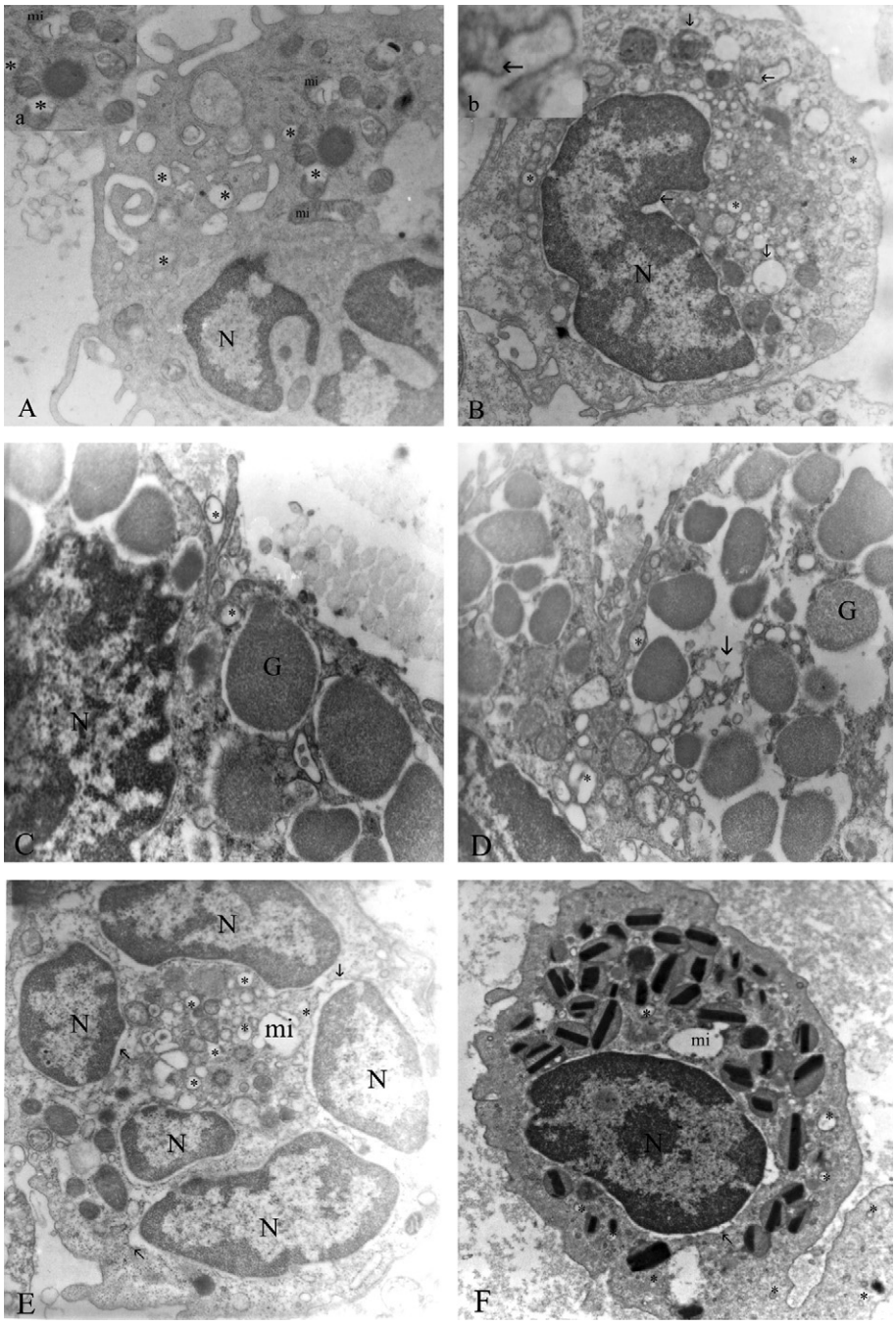

Fig. 4. Transmission electron microscopy of rat peritoneal exudate cells containing psoralen A-loaded nanoparticles (NP), in the absence and presence of light irradiation: (A) macrophage cell with NP (*) without light irradiation; N = nucleus; ±6500× magnification; (B) macrophage cell with NP (*) and light irradiation; N = nucleus; (→) photodamage observed through swelling of the nucleus membrane and mitochondrial damage; ±8000× magnification; (C) mast cell with NP (*) without light irradiation; N = nucleus; G = granule; ±12,000× magnification; (D) mast cell with NP (*) and light irradiation; N = nucleus; G = granule; (→) photodamage observed through swelling of the nucleus membrane and severe mitochondrial damage; ±6300× magnification; (E) leukocyte neutrophil with NP (*) and light irradiation; N = nucleus; (→) photodamage observed through swelling of the nucleus membrane and mitochondrial damage; ±6500× magnification; (F) leukocyte eosinophil with NP (*) and light irradiation; N = nucleus; (→) photodamage observed through swelling of the nucleus membrane and mitochondrial damage; ±6500× magnification.

(64 ± 7%) indicated efficient encapsulation of psoralen A into the PLGA NP. In general, efficient encapsulation of hydrophobic drugs, such as psoralen A, into hydrophobic polymers, such as PLGA, is relatively easy because drug loss to the aqueous phase is decreased, which is a behavior opposite to that observed in the case of hydrophilic drugs (Kompella et al., 2001).

Another parameter evaluated in this work was colloidal stability, which was analyzed by measuring the zeta potential of the NP. In the present study, the blank PLGA particles showed to be negatively charged (−1.3 mV at pH 7.4). This negative value can be explained by the presence of residual PVA on the surface of the particles, even after three washings, which affects

the number of carboxylate-end groups. The residual PVA binds to carboxylate end groups of PLGA altering the particle charge which becomes less negative. On the other hand, psoralen A-loaded NP has a zeta potential of +8.3 mV, which normally is related to a stable colloid (Ruan and Feng, 2003). The positive zeta potential value obtained for the psoralen A-loaded NP may be attributed to an almost uniform positive charge density over the molecule of psoralen, which was observed in the mapped potential energy surface calculated from the optimized structure of the drug by quantum mechanical calculation (Machado, 2004). This positive zeta potential indicates that psoralen A may also be located on the external surface of the PLGA nanoparticles. This feature should influence the release of psoralen A to the medium. The pattern observed for the drug release profile (Fig. 3) can be attributed to the burst effect in the initial stage of the release, which takes place due to the dissolution of psoralen A molecules associated with the surface (*i.e.*, molecules that are not entrapped but are adsorbed on the surface of the NP). Alternatively, the pattern could be due to the psoralen A molecules that could be released through pores and channels formed during the NP preparation. This initial release profile reaches 49% after 3 days. The burst release stage is followed by a very much reduced, but still sustained release of psoralen A for up to 7 days. The release of psoralen A from the PLGA nanoparticle was found to be slow, because of the low porosity of the NP. This resulted in a longer distance for the diffusion of psoralen A through the matrix, as well as in a decrease in the permeability of water, leading to slow PLGA degradation. In this step, the complete release of psoralen A molecules near the surface of the NP was observed. However, the drug molecules that were completely entrapped in the PLGA matrix could not be released until the polymer matrix started to lose its integrity as described by Baras et al. (2000).

Rat peritoneal exudates were used for ultrastructural studies because target cells (defense cells such as macrophages, neutrophils, eosynophils, and mast cells) for PUVA therapy can be easily obtained from them. This approach leads to a better result with respect to the ultrastructural localization of these cells, when compared with the same cells present in tissues.

Ultrastructural studies using rat peritoneal exudate cells incubated with PLGA microparticles (1.4 μm) showed that, among all the cellular types present in the exudate, macrophages are the only cell type that was able to phagocyte the microparticles, even when cells with greater ability to phagocyte, such as neutrophils or even eosinophil cells, were present (Gomes et al., 2004). An important aspect observed in this study was the influence of the particle size on phagocytosis; *i.e.*, smaller particles with size in the range of nanometers could be trapped by various cellular types, not only by macrophage cells, after 120 min of incubation with psoralen A-loaded NP. Another difference between the findings reported here and those of other authors (Hawley et al., 1997; Panyam et al., 2003; Kreuter, 2004) might arise from the use of psoralen A-loaded NP, which dismisses the use of opsonization to make them more attractive to cells.

In Fig. 4A it is possible to observe the macrophage cell with psoralen A-loaded NP inside the cytoplasm. The presence of NP could also be detected inside some organelles, particularly the mitochondria. Macrophage cells which are well-known phagocytes, as well as leukocyte neutrophil and eosinophil, are all able to recognize NP, which are preferentially located inside the mitochondria. Another interesting observation was that mast cells, which are not phagocytes, are also able to endocyte NP. This common behavior is characteristic of the formulation of the psoralen A-loaded NP, and not due to cell type (professional phagocyte or not). The preferential mitochondrial location of the loaded NP can be explained by the fact that the inner side of the membrane is negative (180–200 mV) (Smiley et al., 1991), while the psoralen A-loaded NP displays a positive potential (+8.3 mv), leading to an electrostatic attraction. The opposite effect was observed by Bottiroli et al. (1992), who demonstrated that the primary target for Hematoporphyrin (HpD) in cells submitted to PDT was the lysosome. This is because the photosensitizer is negatively charged, which disables the entrance of HpD into the mitochondria.

The photodamage achieved by the use of non-encapsulated δ-aminolevulinic acid (ALA) irradiation dose (3 J/cm^2) as photosensitizer has been shown by TEM, in a cell culture of keratinocyte (PAM 212) subjected to a 4-h incubation with ALA (Radakovic-Fijan et al., 1999). In our work, however, the use of a reduced incubation time (120 min), psoralen A-loaded NP and cell irradiation with 1 J/cm^2 resulted in the same photodamage observed by Sonja Radakovic-Fijan et al. (1999), showing that the use of a DDS did not alter the efficiency of the drug.

The initial photodamage observed by TEM in our case showed there was damage of the nuclear membrane in all cell types, and both cytoplasmic vesiculation and mitochondrial (partial/total) destruction also occurred. According to Ma et al. (2002), both swelling of the nuclear membrane and condensation of chromatin were observed when the cell was exposed to light irradiation in the presence of 8-MOP (a typical psoralen). In our protocol, photodamage due to psoralen A could be seen in the ultrastructure analysis; however, morphological features of apoptosis, such as chromatin condensation at the nuclear periphery, which are prominent in the PUVA-treated cell, were not observed.

5. Conclusions

In this work, we have shown that entrapment of the drug in the nanoparticle successfully promoted efficient photodamage in the cells (PUVA therapy).

Nanoparticles with characteristics described in this study are an attractive polymeric drug carrier system. They exhibited good level of drug incorporation, which was as high as 64%. These nanoparticles have a zeta potential of +8.3 mV, a value that is considered to be due to a stable colloidal environment. The PLGA nanoparticles were phagocyted by the target cells of PUVA therapy; *i.e.*, neutrophils (No), eosynophils (Eo), and macrophages (Mc), all of them located inside the mitochondria. After PUVA treatment, cell damage was evident from nuclear membrane swelling, cytoplasmic vesiculation, and mitochondria destruction. The great advantage of using psoralen A-loaded NP is the fact that NP are preferentially located inside the mito-

chondria (organelle target), which is the main energy source of the cell. The preferential location of the NP in the mitochondria might improve the therapeutic efficacy of psoralen A because the mitochondria is being the energetic center of the cell. After photodamage, the increase in reactive oxygen species (ROS) inside the mitochondria (once the NP is located inside) should promote increasing oxidative stress, thus leading to cell death.

Acknowledgements

This study was partly supported by CNPq and FAPEMIG Grants (nos. 303911/2003-4, 302679/2002-2 and CEX 85/02). The authors wish to thank Ms. Monika Iamondi and Mr. Antonio Teruyoshi Yabuky, from the Laboratory of Electronic Microscopy, ICB, UNESP, Rio Claro, SP, Brazil for technical assistance.

References

Alleman, E., Leroux, J., Gurny, R., 1998. Polymeric nano and microparticles for the oral delivery of peptides and peptidomimetics. Adv. Drug Deliv. Rev. 34, 171–183.

Baras, B., Benoit, M.A., Gillard, J., 2000. Influence of various technological parameters on the preparation of spray-dried poly(epsilon-caprolactone) microparticles containing a model antigen. J. Microencapsul. 17, 485–498.

Bottiroli, G., Croce, A.C., Ramponi, R., Vaghi, P., 1992. Distribution of disulfonate aluminum phthalocyanine an Photophrin II in living cells: a comparative fluorometric study. Photochem. Photobiol. 55, 575–585.

Canton, M., Caffieri, S., Dall' Acqua, F., Di Lisa, F., 2002. PUVA-induced apoptosis involves mitochondrial dysfunction caused by the opening of the permeability transition pore. FEBS Lett. 522, 168–172.

Carter, D.M., McMacken, M.L.V., Condit, E.S., 1973. Defense of cutaneous cells against UV irradiation. I. Photomediated binding of trimethyl psoralen to DNA of melanoma cells in culture. J. Invest. Dermatol. 60, 270–273.

Chen, W., Lu, R., 1999. Carboplatin-loaded PLGA microspheres for intracerebral injection: formulation and characterization. J. Microencapsul. 16, 551–563.

Cohen, S.R., Burkholder, D.E., Varga, J.M., Carter, D.M., Bartholomew, J.C., 1981. Cell cycle analysis of cultured mammalian cells after exposure to 4,5′,8-trimethylpsoralen and long-wave ultraviolet light. J. Invest. Dermatol. 76, 409–413.

Collins, P., Wainwrigth, N.J., Amorin, N., Lakshmipathi, T., Fergusson, J., 1996. 8-MOP PUVA for psoriasis: a comparison of minimal phototoxic dose-based regime with a skin-type approach. Br. J. Dermatol. 135, 248–256.

Edelson, R.L., 1990. Treatment of cutaneous T-cell lymphoma. Curr. Prob. Dermatol. 19, 226.

Gomes, A.J., Lunardi, L.O., Marchetti, J.M., Lunardi, C.N., Tedesco, A.C., 2005. Photobiological and ultrastructural studies of nanoparticle of poly(lactic-*co*-glycolic acid)-containing bacteriochlorophyll-a as a photosensitizer useful for PDT treatment. Drug Deliv. 12, 159–164.

Gomes, A.J., Faustino, A.S., Lunardi, C.N., Lunardi, L.O., Rigoletto, T.P., Zaniquelli, M.E.D., Machado, A.E.H., 2006. Characterization of PLGA microparticles as a drug carrier for 3-ethoxycarbonyl-2*H*-benzofuro[3,2-*f*]-1-benzopyran-2-one. Ultrastructural study of cellular uptake and intracellular distribution. Drug Deliv. 13, 447–454.

Hawley, A.E., Illum, L., Davis, S.S., 1997. Lymph node localization of biodegradable nanospheres surface modified with poloxamer and poloxamine block copolymers. FEBS Lett. 400, 319–323.

Kompella, U.B., Bandi, N., Ayalasomayajula, S.P., 2001. Poly(lactic acid) nanoparticles for sustained release of budesonide. Drug Deliv. Technol. 1, 28–34.

Kreuter, J., 2004. Influence of the surface properties on nanoparticle-mediated transport of drugs to the brain. J. Nanosci. Nanotechnol. 4, 484–488.

Lacasse, F.X., Fillion, M.C., Phillips, N.C., Escher, E., McMullen, J.N., Hildgen, P., 1998. Influence of surface properties at biodegradable microsphere surfaces: effects on plasma protein adsorption and phagocytosis. Pharm. Res. 15, 312–317.

Legat, F.J., Wolf, P., Kränke, B., 2001. Anaphylaxis to 5-methoxypsoralen during photochemotherapy. Br. J. Dermatol. 145, 821–822.

Lindelöf, B., Sigurgeirsson, B., Tegner, E., Larkö, O., Johannesson, A., Berne, B., Ljunggren, B., Andersson, T., Mollin, L., Nylander-Lundqvist, E., Emtestam, L., 1999. PUVA and cancer risk: the Swedish follow-up study. Br. J. Dermatol. 141, 108–112.

Llano, J., Raber, J., Eriksson, L.A., 2003. Theoretical study of phototoxic reactions of psoralens. J. Photochem. Photobiol. A: Chem. 154, 235–243.

Lysenko, E.P., Melnikova, V.O., Andina, E.S., Wunderlich, S., Pliquett, F., Potapenko, A.Y., 2000. Effects of glutathione peroxidase and catalase on hemolysis and methemoglobin modifications induced by photooxidized psoralen. J. Photochem. Photobiol. B: Biol. 56, 187–195.

Ma, W., Wlaschek, M., Hommel, C., Schneider, L.-A., Scharffetter-Kochanek, K., 2002. Psoralen plus UVA (PUVA) induced premature senescence as a model for stress-induced premature senescence. Exp. Gerontol. 37, 1197–1201.

Machado, A.E.H., 2004. Presentation in VIII Congresso Latinoamericano de Fotoquímica y Fotobiologia (ELAFOT), La Plata, Argentina (Personal Communication).

Machado, A.E.H., Miranda, J.A., Oliveira-Campos, A.M.F., Severino, D., Nicodem, D.E., 2001. Photophysical properties of two new psoralen analogs. J. Photochem. Photobiol. A: Chem. 146, 75–81.

Makki, S., Muret, P., Said, A.M., Bassignot, P., Humbert, P., Agache, P., Millet, J., 1996. Percutaneous absorption of three psoralens commonly used in therapy: effect of skin occlusion (in vitro study). Int. J. Pharm. 133, 245–252.

Man, I., Dawe, R.S., Ferguson, J., Ibbotson, S.-H., 2004. The optimal time to determine the minimal phototoxic dose in skin photosensitized by topical 8 methoxypsoralen. Br. J. Dermatol. 151, 179–182.

Mariano, T.M., Vetrano, A.M., Gentile, S.L., Heck, D.E., Whittemore, M.S., Guillon, C.D., Jabin, I., Rapp, R.D., Heindel, N.D., Laskin, J.D., 2002. Cell-impermeant pyridinium derivatives of psoralens as inhibitors of keratinocyte growth. Biochem. Pharmacol. 63, 31–39.

Middelkamp-Hup, M.A., Pathak, M.A., Parrado, C., Garcia-Caballero, T., Rius-Díaz, F., Fitzpatrick, T.B., González, S., 2004. Orally administered Polypodium leucotomos extract decreases psoralen-UVA-induced phototoxicity, pigmentation, and damage of human skin. J. Am. Acad. Dermatol. 50, 41–49.

Okamoto, H., Guo, Z., Imamura, S., 1993. In vitro granuloma formation by spleen cells treated with psoralen plus long-wave ultraviolet radiation. Photochem. Photobiol. 57, 667–669.

Oliveira, A.M.A.G., Raposo, M.M.M., Oliveira-Campos, A.M.F., Machado, A.E.H., 2003. Synthesis of psoralen analogues based on dibenzofuran. Helv. Chim. Acta 86, 2900–2907.

Panyam, J., Labhasetwar, V., 2003. Biodegradable nanoparticles for drug and gene delivery to cells and tissue. Adv. Drug Deliv. Rev. 55, 329–347.

Panyam, J., Sahoo, S.K., Prabha, S., Bargar, T., Labhasetwar, V., 2003. Fluorescence and electron microscopy probes for cellular and tissue uptake of poly(D,L-lactide-*co*-glycolide) nanoparticles. Int. J. Pharm. 262, 1–11.

Panyam, J., Zhou, W.-Z., Prabha, S., Sahoo, S.K., Labhasetwar, V., 2004. Rapid endo-lysosomal escape of poly(DL-lactide-coglycolide) nanoparticles: implications for drug and gene delivery. FASEB J. 16, 1217–1226.

Pires, A.L., Honda, N.K., Cardoso, C.A.L., 2004. A method for fast determination of psoralens in oral solutions of phytomedicines using liquid chromatography. J. Pharm. Biomed. Anal. 36, 415–420.

Radakovic-Fijan, S., Rappersberger, K., Tanew, A., Hönigsmann, H., Ortel, B., 1999. Ultrastructural changes in PAM cells after photodynamic treatment with delta-aminolevulinic acid-induced porphyrins or photosan. J. Invest. Dermatol., 112.

Roop, S., Guy, J., Berl, V., Bischoff, P., Lepoittevin, J.-P., 2004. Synthesis and photocytotoxic activity of new α-methylene-χbutyrolactone-psoralen heterodimers. Bioorg. Med. Chem. 12, 3619–3625.

Ruan, G., Feng, S.-S., 2003. Preparation and characterization of poly(lactic acid)–poly(ethyleneglycol)–poly(lactic acid) (PLA–PEG–PLA) microspheres for controlled release of paclitaxel. Biomaterials 24, 5037–5044.

Saiad, A., Makki, S., Muret, P., Humbert, P., Millet, J., 1997. Psoralens percutaneous permeation across the human whole skin and the epidermis in respect to their polarity (in vitro study). J. Dermatol. Sci. 14, 136–144.

Smiley, S.T., Reers, M., Mottola-Hartshorn, C., Lin, M., Chen, A., Smith, T.W., Steele Jr., G.D., Chen, L.B., 1991. Intracellular heterogeneity in mitochondrial membrane potentials revealed by a J-aggregate-forming lipophilic cation JC-1. Cell Biol. 88, 3671–3675.

Tatchen, J., Kleinschmidt, M., Marian, C.M., 2004. Electronic excitation spectra and singlet-triplet coupling in psoralen and its sulfur and selenium analogs. J. Photochem. Photobiol. A: Chem. 167, 201–212.

Tokura, Y., 1999. Modulation of cytokine production by 8-methoxypsoralen and UVA. J. Dermatol. Sci. 19, 114–122.